Reduction of Sintering during Annealing of FePt Nanoparticles Coated with Iron Oxide

Chao Liu,[†] Xiaowei Wu, Timothy Klemmer,* Nisha Shukla, and Dieter Weller

Seagate Research, 1251 Waterfront Place, Pittsburgh, Pennsylvania 15222-4215

Anup G. Roy, Mihaela Tanase, and David Laughlin

Data Storage Systems Center, Carnegie Mellon University, Pittsburgh, Pennsylvania 15213

Received May 25, 2004. Revised Manuscript Received October 12, 2004

FePt/iron oxide core/shell nanoparticles are synthesized by a two step polyol process with 1,2-hexadecanediol as the reducing reagent. Monodispersed 2.6-nm FePt nanoparticles are first obtained by reduction of iron(III) acetylacetonate and platinum(II) acetylacetonate. These preformed FePt nanoparticles are then used as seeds and an iron oxide shell is formed in the second synthesis step. The role of the iron oxide shell on sintering of FePt nanoparticles is investigated. Annealing studies show that these FePt/iron oxide core/shell structures are stable after annealing at 550 °C for 30 min at which 2.6-nm FePt nanoparticles without oxide shell coating start to sinter. Low-temperature magnetic hysteresis behavior of the annealed core/shell nanoparticles suggests exchange coupling between the magnetically hard FePt core and the magnetically soft iron oxide shell.

Introduction

Chemically ordered CoPt and FePt alloys with the $L1_0$ crystalline phase are key candidates for future-generation ultrahigh-density magnetic recording media, due to their enhanced magnetocrystalline anisotropy and potential for small thermally stable grains.[1] Chemical synthesis routes have been used to demonstrate monodispersed FePt nanoparticles,[2] and self-organized arrays of $L1_0$ FePt nanoparticles have been proposed as alternative magnetic recording media. One of the main obstacles to implementing such media is sintering, which destroys the particle array order. Sintering occurs as a result of annealing, which is needed to transform the as-made nanoparticles into the chemically ordered $L1_0$ phase.

Sintering takes place at annealing temperatures above about 350−400 °C, when the surfactant molecules encapsulating the FePt nanoparticles decompose and the adjacent particles start to agglomerate. Sintering is strongly influenced by the kinetic diffusion mechanism between particles and the thermodynamic surface energy of the particles. One strategy to inhibit interparticle diffusion and sintering is to coat the particles with diffusion barrier materials. Putting new materials on the surface as a shell can greatly modify diffusion rates and surface energies while keeping the desirable properties of the core material. The FePt alloy in the core must not be degraded during the shell coating process. For example, there should be no reaction between the core materials and shell materials during the annealing process at elevated temperatures, which are needed for the $L1_0$ phase transformation. If magnetic materials are used as the shell, magnetic interactions between the core and shell materials also must be considered. Other concepts such as increasing anisotropy by magnetic exchange coupling between ferromagnetic and antiferromagnetic materials can also be utilized for the design of core/shell nanoparticles.[3]

Previously, bimagnetic core/shell FePt/Fe_3O_4 particles have been considered for fabrication of magnetic nanocomposites with enhanced energy product, and the 4-nm FePt core is synthesized by simultaneous thermal decomposition of iron pentacarbonyl and polyol reduction of platinum salt.[4] However, there are disadvantages associated with iron pentacarbonyl which arise from its physical nature. Iron pentacarbonyl is highly toxic, and a flammable liquid at room temperature. In addition to the safety handling concerns, the stoichiometry of the FePt particles is difficult to control using this process. This is due to the fact that the reaction temperature is above the boiling point of 103 °C of iron pentacarbonyl, therefore some of the iron is lost and not incorporated into the FePt alloy nanoparticles.[5] Meanwhile, the polyol process that utilizes diol or polyalcohol to synthesize metal particles has demonstrated to be a good approach to obtaining FePt as well as iron oxide nanoparticles.[6−10] In this work, we focus on synthesizing monodispersed 2.55-

* To whom correspondence should be addressed. E-mail: timothy.j.klemmer@seagate.com.
† Current address: Nanosys Inc., 2625 Hanover St., Palo Alto, CA 94304.
(1) Weller, D.; Moser, A. *IEEE Trans. Magn.* **1999**, *35*, 4423.
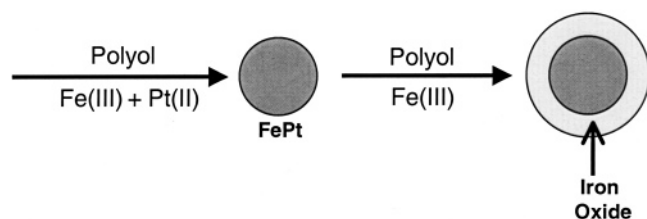(2) Sun, S.; Murray, C. B.; Weller, D. *Science* **2000**, *287*, 1989.

(3) Skumryev, V.; Stoynov, S.; Zhang, Y. *Nature* **2003**, *423*, 850.
(4) Zeng, H.; Li, J.; Wang, Z. L.; Liu, J. P.; Sun, S. *Nano. Lett.* **2004**, *4*, 187.
(5) Sun, S.; Weller, D. *J. Magn. Soc. Jpn.* **2001**, *25*, 1434.
(6) Liu, C.; Wu, X.; Klemmer, T. J.; Shukla, N.; Yang, X.; Weller, D.; Roy, A. G.; Tanase, M.; Laughlin, D. *J. Phys. Chem. B* **2004**, *108*, 6121.

Figure 1. Schematic drawing for the overall process to synthesize core/shell FePt/iron oxide nanoparticles.

nm FePt nanoparticles through a polyol process. Then an iron oxide shell is grown on the preformed FePt core based on a heterogeneous seeded growth reaction through another polyol process. In our experiments both FePt alloy and iron oxide nanoparticles have been obtained through polyol process with the same reducing reagent, 1,2-hexanedecanediol. Typically, it is considered difficult to reduce Fe salt in a polyol process.[11] However, it is reported that Pt cations can play a critical role in inducing and accelerating the reduction of associated metal cations.[8−9] Therefore, Fe salt can be reduced to the neutral state and FePt alloy particles are obtained when both Fe salt and Pt salt are involved in the reactions. If there is only iron salt in the reaction system to be reduced, magnetite Fe_3O_4 nanoparticles have been obtained by others,[10] which is also consistent with our second polyol process for making the iron oxide shell. The influence of the iron oxide shell coating on sintering of FePt nanoparticles is investigated.

Experimental

All chemicals were used as received. Platinum (II) acetylacetonate (99.99%), iron (III) acetylacetonate (99.95%), oleic acid (90%, tech.), oleylamine (70%, tech.), octyl ether (99%), phenyl ether (99%), anhydrous ethyl alcohol, and hexane were ordered from Sigma-Aldrich. 1,2-Hexanedecanediol (90%, tech.) was ordered from Fluka. The overall process is schematically shown in Figure 1. In the first stage, Fe (III) and Pt (II) cations were reduced to FePt alloy through a polyol process. Then Fe(III) and 1,2-hexanedecanediol (excluding Pt) were used in a second polyol process to grow an iron oxide shell upon the preformed FePt seeds.

A typical experiment for the polyol process synthesis of monodispersed FePt nanoparticles began with mixing stoichiometric amounts of platinum (II) acetylacetonate (0.5 mmol) and iron (III) acetylacetonate (0.5 mmol), reducing reagent 1,2-hexanedecanediol (5 mmol), oleic acid (0.5 mmol), and oleylamine (0.5 mmol), in 20.0 mLof octyl ether solution at room temperature. The solution was then heated to reflux at 286 °C and kept at this temperature for 30 min. Afterward, the heat source was removed and the product solution was allowed to cool to room temperature. The particles were then purified by centrifugation after a flocculent, e.g., ethyl alcohol, was added. The supernatant solution was discarded and the precipitates were dispersed into 10.0 mL of nonpolar solvent such as hexane, in the presence of oleic acid and oleylamine.

Then un-annealed polyol-synthesized FePt nanoparticles are used as seeds for an iron oxide shell to be grown upon them through

another polyol process. This polyol process, based on a heterogeneous seeded-growth mechanism,[12] involves iron (III) acetylacetonate and 1,2-hexanedecanediol. Experimental conditions are controlled well so that additional homogeneous nucleation of new particles can be avoided, and all growth occurs upon the preformed seeds. The reaction temperature, concentration of seeds, and concentration of newly added chemical reagents were considered. The thickness of the iron oxide shell was controlled by the relative amounts of the preformed particles and newly added iron salt. A typical experiment started with 5.0 mL of hexane solution of the preformed FePt nanoparticles together with 0.5 mmol Fe (III) acetylacetonate, 3 mmol 1,2-hexanedecanediol, and 20.0 mL of phenyl ether put into the reaction flask. Hexane was removed by evaporation when the temperature was above its boiling point of 67 °C. Then the mixture was heated to reflux at 259 °C and dwelled at this temperature for 30 min. After the heating source was removed and the reaction mixture was allowed to cool, the particle solution was purified by centrifugation after the addition of a flocculent (ethyl alcohol in this case) and dispersed into nonpolar solvent (hexane) with desired concentrations.

TEM samples were prepared by evaporating a drop of the particle solution deposited onto the carbon-coated TEM grids. Samples for XRD and magnetic measurements were obtained by evaporating FePt particle hexane dispersions on thermally oxidized Si wafers. The annealing was achieved using a rapid thermal processor (RTP) in Ar atmosphere, where the oxygen level during annealing was kept to less than 1 ppm. X-ray diffraction (XRD) studies of the annealed samples were carried out using a Philips X'PERT PRO MRD equipped with an X-ray mirror using primarily asymmetric glancing incidence scans with the incident angle set at 3 degrees. Conventional TEM studies are carried out using a Philips EM420T microscope operating at 120 kV. High-resolution TEM (HRTEM) studies are performed using a Philips TECNAI microscope with an operating voltage of 200kV and a point resolution of 2.1Å. Magnetic properties were studied with a Quantum Design MPMS XL Superconducting Quantum Interference Device (SQUID) magnetometer.

Results and Discussion

The monodispersity of FePt nanoparticles synthesized via the polyol process is verified by TEM studies. Figure 2a shows a representative bright field TEM image of an as-prepared FePt nanoparticle sample. Figure 2b shows a particle size analysis based on a log-normal distribution. The analysis indicates monodispersity with an average diameter of 2.55 nm and a standard deviation of 0.23 nm. The chemically disordered nature of FePt nanoparticles is confirmed with the identification of fcc FePt (111) and (200) planes in the HRTEM image shown in Figure 2c. The image shows that the particles have uniform lattice fringes across the particles, which is attributed to good crystallinity. These TEM results are similar to respective results from as-prepared FePt nanoparticles using iron pentacarbonyl chemistry.[13−14] The composition of polyol synthesized FePt alloy nanoparticles was studied by XRD after annealing.[15] An XRD pattern of nanoparticles annealed at 650 °C for 30 min is shown in Figure 3a, and the chemically ordered $L1_0$ crystal structure

(7) Elkins, K. E.; Vedantam, T. S.; Liu, J. P.; Zeng, H.; Sun, S.; Ding, Y.; Wang, Z. L. *Nano Lett.* **2003**, *3*, 1647.
(8) Jeyadevan, B.; Hobo, A.; Urakawa, K. *J. Appl. Phys.* **2003**, *93*, 7574.
(9) Jeyadevan, B.; Urakawa, K.; Hobo, A. *Jpn. J. Appl. Phys.* **2003**, *42*, L350.
(10) Sun, S.; Zeng, H. *J. Am. Chem. Soc.* **2002**, *124*, 8204.
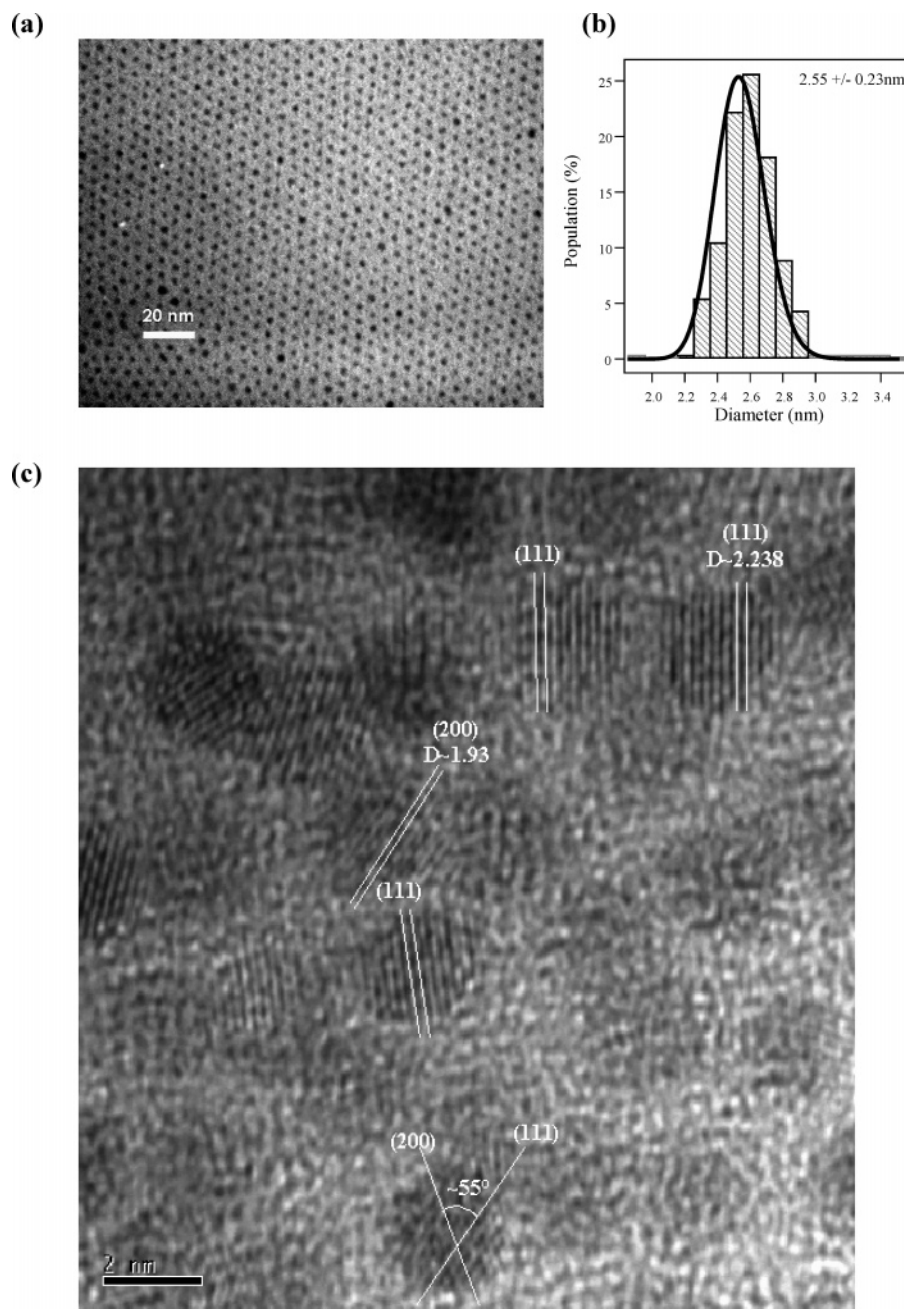(11) Viau, G.; Fievet-Vincent, F.; Fievet, F. *J. Mater. Chem.* **1996**, *6*, 1047.

(12) Yu, H.; Gibbons, P. C.; Kelton, K. F.; Buhro, W. E. *J. Am. Chem. Soc.* **2001**, *123*, 9198.
(13) Dai, Z. R.; Sun, S.; Wang, Z. L. *Nano. Lett.* **2001**, *1*, 443−447.
(14) Dai, Z. R.; Wang, Z. L.; Sun, S. *Surf. Sci.* **2002**, *505*, 325.
(15) Klemmer, T. J.; Shukla, N.; Liu, C. *Appl. Phys. Lett.* **2002**, *81*, 2220.

**(a)**

(b)

(c)

Figure 2. TEM bright field image of as-prepared FePt nanoparticles on the carbon-coated copper grid (a). The particles are monodispersed with 2.55-nm diameter and standard deviation as 0.23 nm (b). Curve fitting is based on the assumption of log-normal distribution. High-resolution TEM image suggested chemically disordered fcc phase. Identification of random lattice fringes for fcc FePt (111) and (200) planes indicates that the particles are randomly oriented on the TEM grid (c).

is present. To measure the lattice parameters (both c and a), the superlattice peaks of (001) and (110) are fitted and used to calculate the c-parameter and a-parameter, respectively. Additionally, the (200)/(002) peak is de-convoluted and used to calculate the c and a lattice parameters. Profile fitting of the superlattice (001) and (110) peaks of the X-ray diffraction pattern reveals the lattice constants $a = 3.861$ Å and $c = 3.724$ Å, with $c/a = 0.965$. When fitting the fundamental (200)/(002) peaks we calculate $a = 3.867$ Å, $c = 3.737$ Å, and $c/a = 0.966$. This is consistent with the lattice constants for near equiatomic fully chemically ordered FePt with $L1_0$ phase.[15] Magnetic in-plane hysteresis measurements (Figure 3b) show a coercivity (Hc) of 23.1 kOe at 5 K for the annealed FePt nanoparticles, indicating that FePt nanopar-

ticles with high anisotropy ($L1_0$ phase) have been obtained. Both XRD and magnetic property studies verify that the nanoparticles have a composition near $Fe_{50}Pt_{50}$ within the $L1_0$ phase range.

Some representative TEM images of FePt/iron oxide core/shell nanoparticles with 2.55-nm core/2.5-nm shell are shown in Figure 4a. A uniform shell coating and local self-assembly is observed. An XRD pattern for this sample is shown in Figure 4d; it suggests the coexistence of two crystalline phases: chemically disordered fcc FePt and iron oxide. This is corroborated by the identification of lattice fringes in HRTEM images in Figure 4b and c for fcc FePt (111) planes and iron oxide (220) planes. The crystalline phase of iron oxide cannot be distinguished unambiguously between
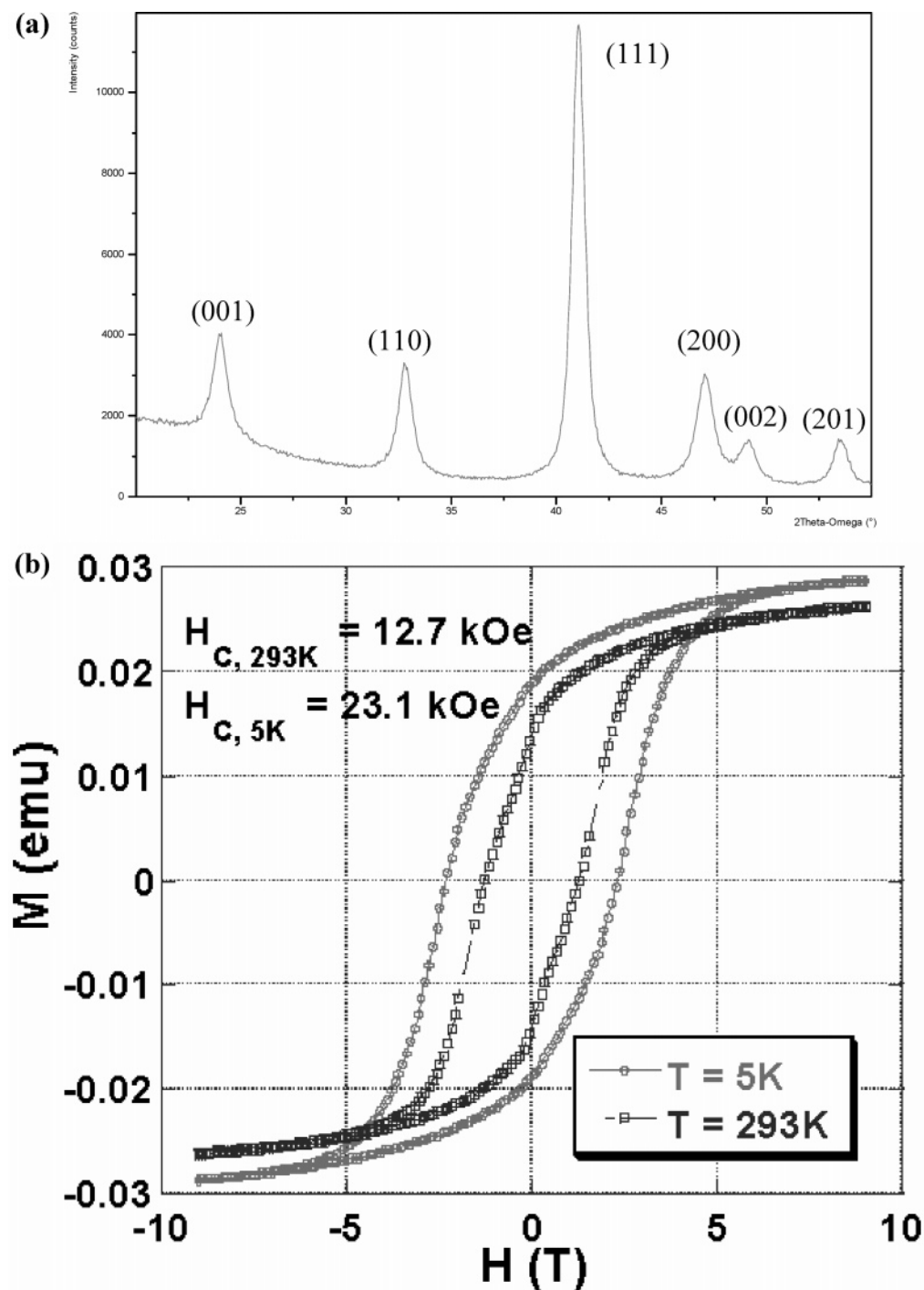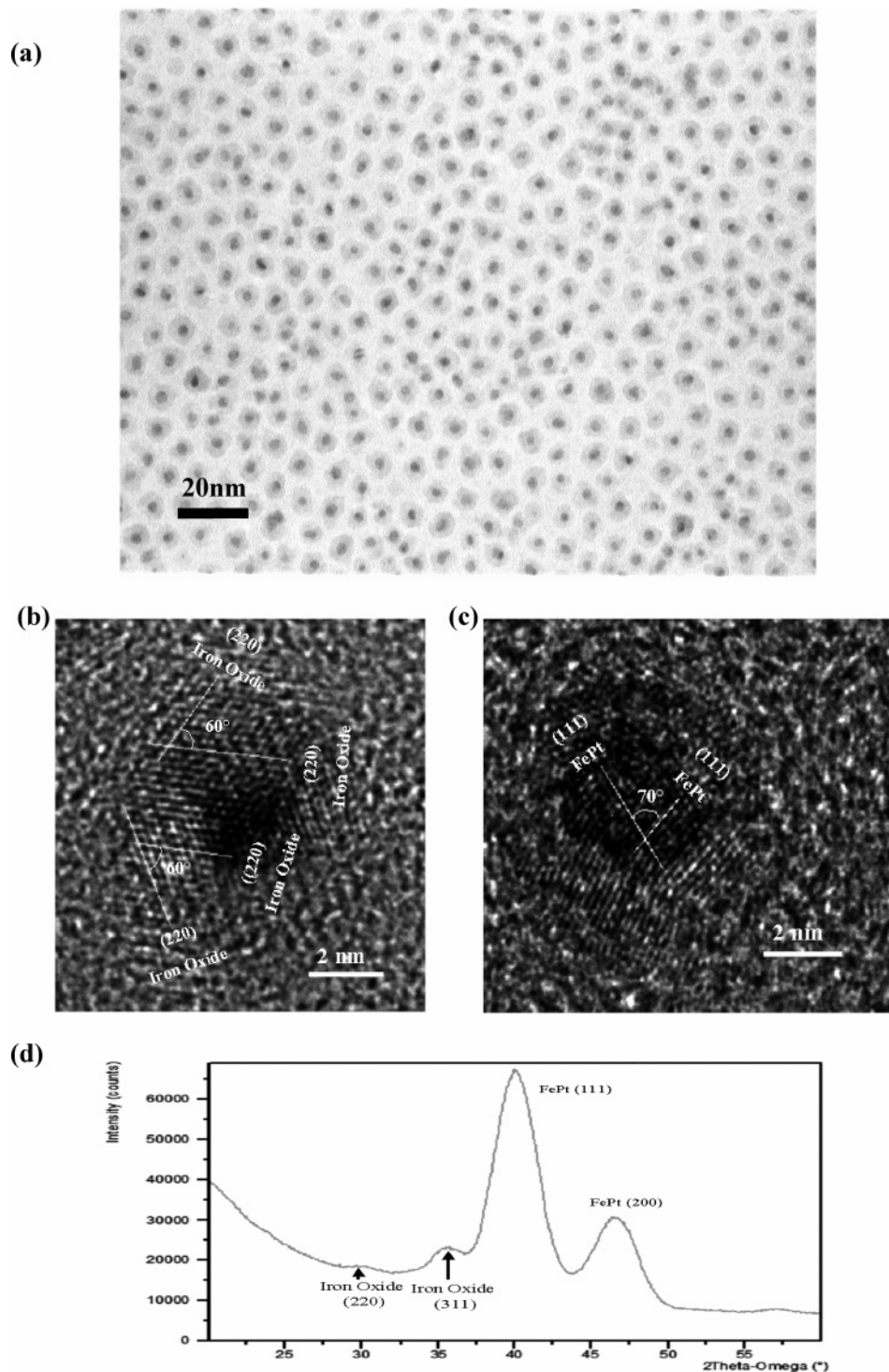
Figure 3. X-ray diffraction pattern of FePt nanoparticles after heat treatment by RTA at 650 °C for 30 min verified the chemically ordered L1$_0$ crystalline structure. Profile fitting of the XRD pattern revealed that *a* is 3.861 Å and *c* is 3.724 Å, with *c/a* ratio 0.965 by fitting the superlattice (001) and (110) peaks; and *a* is 3.867 Å, *c* is 3.737 Å, with *c/a* ratio 0.966 based on the fitting of fundamental (200)/(002) peaks (a). (b) Hysteresis measurements of FePt particles after annealing. Coercivities are 12.7 kOe at 298 K and 23.1 kOe at 5 K.

magnetite Fe$_3$O$_4$ and γ-Fe$_2$O$_3$ because of similar *d* spacings for these two iron oxides.

The surface properties are then mainly determined by the iron oxide at the surface after the shell-coating process. The role of the iron oxide shell in preventing sintering is verified by annealing the FePt/iron oxide core/shell nanoparticles at 550 °C for 30 min. Figure 5a shows an XRD pattern of the annealed FePt/iron oxide core/shell nanoparticles at 550 °C for 30 min. The broad peak at 35.5° is associated with the iron oxide. The observation of the broad superlattice (001)

peak at 23.8° verifies the transformation to the L1$_0$ phase. However, a (110) superlattice peak is not clearly observed in the XRD pattern, which may be ascribed to the broad intensity and overlapping with the background contributions of the oxide. The annealing partially transformed the chemically disordered FePt in the core to the chemically ordered L1$_0$ phase. To measure the lattice parameters of the annealed FePt/iron oxide core/shell nanoparticles annealed at 550 °C for 30 min, the fundamental (200)/(002) peak is de-convoluted and used to calculate the *c* and *a* lattice

Figure 4. TEM bright field image of as-prepared FePt/iron oxide core/shell nanoparticles (a). High-resolution TEM images (b and c) suggest chemically disordered fcc phase in the core and iron oxide at the shell. (d) X-ray diffraction patterns of as-prepared FePt/iron oxide core/shell nanoparticles verify the existence of chemically disordered FePt and iron oxide.

parameters. Profile fitting reveals the lattice constants $a = 3.871$ Å and $c = 3.762$ Å, with $c/a = 0.972$. This may suggest that the complete ordering to $L1_0$ is not obtained yet for annealing at 550 °C for 30 min. The mean grain size for the annealed sample determined from the peak broadening of the (111) peak in the in-plane XRD pattern by using the Scherrer equation (assuming spherical shapes) is about 2.6 nm, while the mean size for the as-prepared sample is 2.5 nm. Annealing at 550 °C for 30 min has hence almost no

effect on the average size of FePt alloy in the core. The TEM image in Figure 5b demonstrates that FePt/iron oxide core/ shell nanoparticles are stable up to 550 °C for 30 min whereas regular FePt nanoparticles are observed to sinter. The role of the oxide shell on sintering prevention is parallelly verified by annealing the 2.55-nm FePt nanoparticles without the oxide shell coating at the same conditions, i.e., 550 °C for 30 min. As sintering of FePt nanoparticles on substrates strongly depends on size, bonding to substrate,
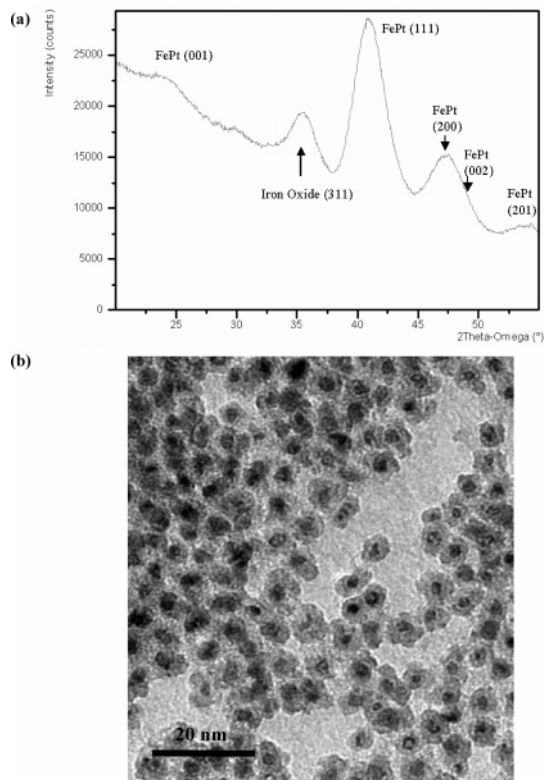
Figure 5. TEM bright field image of FePt/iron oxide core/shell nanoparticles annealed at 550 °C for 30 min (a). The core/shell structures are stable up to 550 °C for 30 min. No significant sintering is observed. (b) X-ray diffraction pattern of FePt/iron oxide core/shell nanoparticles after annealing at 550 °C for 30 min. Superlattice (001) peak is observed.

and surfactant molecule shell, etc., the 2.55-nm FePt particles are purified and dispersed in hexane with controlled surfactant amounts and deposited on the thermally oxidized Si wafer in exactly the same fashion as FePt/iron oxide core/shell nanoparticles. Figure 6 shows the annealed particles without oxide shell coating do not maintain the self-assembly at 550 °C for 30 min, and larger size particles and significant sintering are observed.

Since the magnetic properties of the core and shell materials are significantly different, one would expect to observe strong multiphased structures from the magnetic measurements as well. To avoid the complication of superparamagnetic effects in a system with such small particles, we measure the hysteresis loops at low temperature ($T = 5$ K) using a SQUID magnetometer as shown in Figure 7. The hysteresis loop clearly consists of two parts: a magnetically soft phase (iron oxide at the shell) that is easily switched at low magnetic field, and a gradual slope at high field, indicating the existence of a magnetically hard phase (partially ordered FePt in the core). Comparing with the hard/soft exchange coupled system reported by Sun,[8] our system still shows a distinct two-phase structure with weak exchange coupling between core and shell. By extracting the soft magnetic phase from the overall hysteresis measurements,
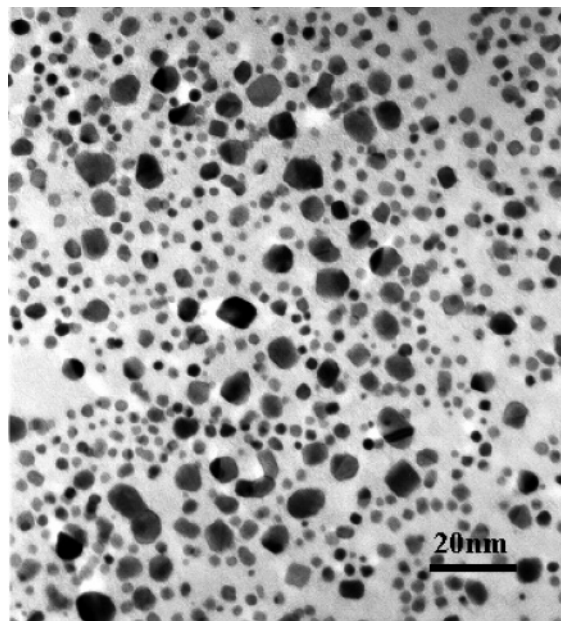
Figure 6. TEM bright field image of 2.55-nm FePt nanoparticles annealed at 550 °C for 30 min.
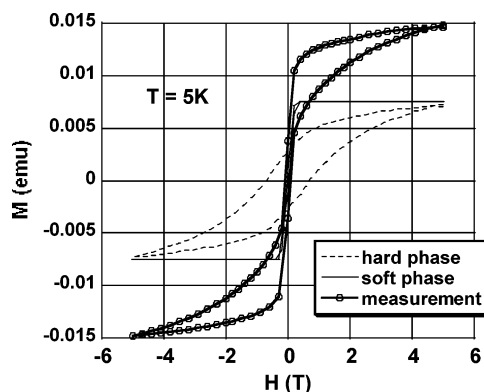
Figure 7. Hysteresis measurements (5 K) of FePt/iron oxide core/shell nanoparticles after annealing at 550 °C for 30 min.

the contribution from the hard phase is obtained. The coercivity of the hard phase is about 7000 Oe at 5 K. This relatively low coercivity is consistent with incomplete chemical ordering of the FePt core. We point out that, if the assumption of nonsintered FePt is true, for a particle size of 2.5-nm diameter, superparamagnetic effects at 5 K are still quite significant. Therefore, the relatively low coercivity at 5 K is at least partially due to superparamagnetic effects.

Annealing of the FePt/iron oxide core/shell structures at 600 °C for 30 min and at 650 °C for 30 min leads to the annihilation of the core/shell structures. This is observed in TEM. It seems that more chemically stable barrier materials need to be applied to minimize sintering during these higher annealing temperatures.